Trojan Exoplanets

Philippe Robutel, Adrien Leleu

Trojan Exoplanets

Philippe Robutel and Adrien Leleu

To be published in: Handbook of Exoplanets, 2nd Edition, Hans Deeg and Juan Antonio Belmonte (Eds. in Chief), Springer International Publishing AG, part of Springer Nature.

Abstract Co-orbital exoplanets are a by-product of the models of formation of planetary systems. However, none have been detected in nature thus far. Although challenging, the observation of co-orbital exoplanets would provide valuable information on the formation of planetary systems as well as on the interactions between planets and their host star. After a brief review of the stability and formation issues of co-orbital systems, some observational methods dedicated to their detection are presented.

Introduction

The existence of Trojans in extrasolar systems has already been discussed in the chapter "Special Cases: Moons, Rings, Comets, and Trojans". The present chapter generalizes this concept by considering co-orbital planets. This kind of configuration consists of a planet pair trapped in the 1:1 mean motion resonance. Thus, con-

Philippe Robutel
IMCCE, Observatoire de Paris, PSL University, CNRS, Sorbonne Université, 77 avenue Denfert-Rochereau, 75014 Paris, France, e-mail: philippe.robutel@obspm.fr

Adrien Leleu
Observatoire de Genève, Université de Genève, Chemin Pegasi, 51, 1290 Versoix, Switzerland, e-mail: adrien.leleu@unige.ch

trary to the Trojan case, discussed in the above-mentioned chapter, for which the mass is supposed to be small enough not to perturb the motion of the two other bodies (restricted case), it is possible to have co-orbital planets of comparable masses provided their sum remains small with respect to the mass of the star (less than 25 times smaller).

Co-orbital configurations are well known in the solar system. More than a century after the pioneer works of (Euler 1764), who discovered the aligned configurations in the general 3-body problem, and Lagrange (1772) who demonstrated the existence of the famous equilateral configurations, was discovered Achilles, the first Trojan asteroid (Wolf 1906). Since then, thousands of small bodies are observed in the Jovian Trojan swarms L_4 and L_5 as well as some Neptune, Uranus, Mars and Earth Trojans (see `https://www.minorplanetcenter.net/iau/lists/Trojans.html`). Saturn's satellite system also hosts co-orbital satellites, in particular the famous Janus and Epimetheus pair which, unlike most Trojans in the solar system, follow horseshoe trajectories of very large amplitude (Dermott and Murray 1981; Thomas et al. 2013).

Although many theoretical works suggest that co-orbital exoplanets may also exist, such a pair of planets has yet to be observed. In particular, out of the hundreds of multi-planetary systems discovered by the Kepler mission, none were found in co-orbital configuration thus far. Although this result points to a relative rarity of the configuration, part of this absence might be due to observational biases.

After reviewing the stability issues of co-orbital systems, the main methods dedicated to their detection will be outlined.

Co-orbital configurations and their stability

The first stability result was established by Gascheau (1843) who proved that the Lagrange equilateral configuration was stable, in the coplanar circular case, providing the masses m_j satisfy the following relation

$$(m_0+m_1+m_2)^2 \geq 27(m_0m_1+m_0m_2+m_1m_2).$$

In order to be satisfied, this condition requires that the mass of one body, for instance m_0, dominates the others. Thus, it can be verified that, the mass ratio $\mu = (m_1+m_2)/m_0$ must remain smaller than 0.04 to ensure stability. Therefore, it is not necessary for one of the masses to be negligible in front of the other two, as is the case with the Jovian Trojans. In particular, there is no reason why a Lagrange configuration consisting of one solar mass star and two Jovian planets should not be stable. These particular periodic solutions being linearly stable, their neighborhoods are filled with quasi-periodic orbits, known as tadpole-orbits, or also trojan-orbits by analogy with the Jovian Trojans , that correspond to small to moderate deformations of the equilateral configurations (Fig. 1, solid lines). Although the Lagrangian triangular equilibria are linearly stable, the overall stability of the tadpole region is not

guaranteed. Indeed, for some particular values of the mass ratio μ associated with resonances, the stability domain shrinks, or even disappears entirely. (e.g. Danby 1964; Giorgilli et al. 1989; Roberts 2002; Nauenberg 2002; Érdi et al. 2007). For a given tadpole orbit, the libration angle ζ, equal to the difference of the planetary mean-longitude λ_1 and λ_2, oscillates around a value close to $\pm 60^\circ$ (depending on whether one considers the L_4 or L_5 neighborhood) with a frequency ν equal to $n\sqrt{27\mu}/2$ very close to Lagrange equilibria, n being the orbital frequency common to the two planets, and remains of the same order throughout the tadpole areas. In case of significant eccentricities, perihelia slowly precess with small secular frequency of order μ, which is therefore small compared to the libration frequency.

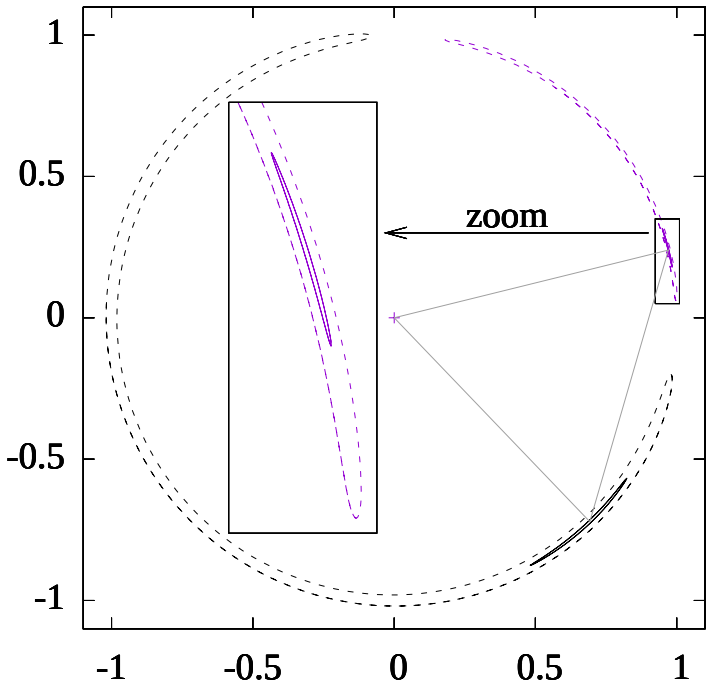

Fig. 1 Tadpole (solid lines) and horseshoe orbits (dashed lines) seen in a rotating frame with the common orbital frequency n of both planets. The coordinates of the central body are $(0,0)$ while while the co-orbital's orbits are plotted in $(a_j\cos(\lambda_j - nt), a_j\sin(\lambda_j - nt))$. The purple orbits correspond to the planet 1 whose mass satisfies $m_1/m_0 = 10^{-4}$ while those of the second planet with $m_2/m_0 = 3\,10^{-5}$ are plotted in purple. The grey equilateral triangle indicates the Lagrange configuration. The initial conditions of the horseshoe orbit satisfy $a_1 = a_2 = 1$, $e_1 = e_2 = 0$, $\lambda_1 - \lambda_2 = \varpi_1 - \varpi_2 = 15^\circ$, while $\lambda_1 - \lambda_2 = \varpi_1 - \varpi_2 = 45^\circ$ is set for tadpole.

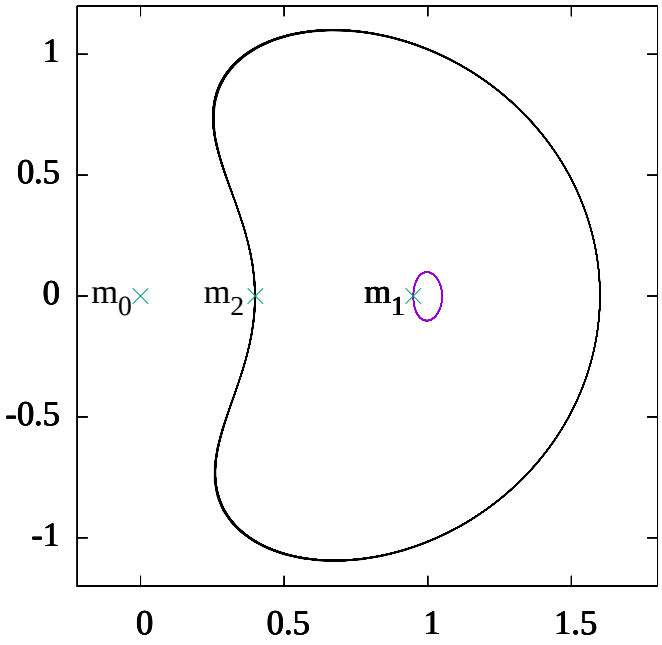

Fig. 2 Quasi-satellite orbit. Trajectory of the first planet (purple) and of the second one (black) seen in a rotating frame with the common orbital frequency n of the both planets. The masses are the same than in Fig. 1, while the initial elliptic elements satisfy $a_1 = a_2 = 1$, $e_1 = 0.05, e_2 = 0.6$.

When μ is lower than a specific value close to 0.0004 (Laughlin and Chambers 2002), the libration angle ζ can undergo variations of much greater amplitude given birth to horseshoe orbits, which become stable below this critical value (Fig. 1, dashed lines). Along horseshoe orbits, the libration angle ζ evolves with an amplitude which is greater that 312°, while for tadpole orbits this amplitude is bounded by 156°. As with the tadpole orbits, the coplanar dynamic is driven by three distinct time scales: the fast one, related to the orbital period; the semi-fast, associated with the libration inside the 1:1 mean-motion resonance, and the secular related to orbital precession. For large eccentricities, the width of the tadpole and horseshoe domains shrink to make room for quasi-satellites orbits (Giuppone et al. 2010; Pousse et al. 2017). Other families of orbits also exist for highly eccentric orbits (Leleu et al. 2018). As it is the case in the solar system, it can also be assumed that the orbits of the two co-orbital are not coplanar. If the mutual inclination is low, the main dynamical features are very similar to those described above. Higher inclinations allow transitions between theses different types of orbits and merging between them (Namouni 1999), but in any case, the mutual inclination of stable co-orbital tadpole-orbits may not exceed about 60° degrees (see Qi and de Ruiter 2020). Other kinds of

trajectories, which are not discussed here, also exist within the co-orbital resonance such as retrograde motions (Morais and Namouni 2016; Sidorenko et al. 2014).

When the co-orbital bodies are embedded in a multi-planetary system, the dynamics become much more complex and the size of the stability regions may decrease significantly. Because of the additional fundamental frequencies associated with the whole planetary system (three frequencies per planet) a wide range of resonances can destabilize the coorbital system (Marzari et al. 2003; Robutel and Gabern 2006; Leleu et al. 2019b). These phenomena have many consequences. They are the cause of the slow erosion of the Jovian Trojan swarms (Levison et al. 1997; Robutel and Gabern 2006), they introduce unstable areas in the tadpole and horseshoe regions (Leleu et al. 2019b), and can go so far as to make the whole coorbital region unstable, as is the case with Saturn (Holman and Wisdom 1993; Nesvorny and Dones 2002; Hou et al. 2014).

Formation and evolution of co-orbital exoplanets

To understand the particularities of the co-orbital resonance, it is useful to recall the current understanding for the formation and evolution of other resonant configurations.

First and second-order MMRs are natural and common outcomes of models of formation of planetary systems: as planets form in the protoplanetary disc, they tend to migrate toward the star. Depending on their relative migration speed and eccentricities, they have a probability of being captured in each of the MMRs they cross (e.g. Lee and Peale 2002), the most commonly observed being the 3:2 MMR. Models hence predict that toward the end of the protoplanetary disc phase, numerous planetary systems are in close-in, compact resonant state (e.g. Cresswell and Nelson 2008; Coleman et al. 2019; Emsenhuber et al. 2021). As the protoplanetary disc dissipates, the eccentricity damping lessens, which can lead to instabilities (e.g. Terquem and Papaloizou 2007; Pu and Wu 2015; Izidoro et al. 2017). For planets that remained in resonance, and are close enough to their host star, tides become the dominant force that affect the architecture of the systems, which can then lead to a departure of the period ratio from the exact resonance (Henrard and Lemaitre 1983; Papaloizou and Terquem 2010; Delisle et al. 2012). This succession of dissipative processes partly explain why the observed close-in multi-planetary systems are often just outside MMRs, but rarely inside (Fabrycky et al. 2014).

Both of the aforementioned phenomenon, i.e. the smooth convergent migration in resonance during the protoplanetary disc, and the slow departure from resonance due to tides, cannot be applied to the co-orbital resonance. Indeed, this resonance is surrounded by a chaotic area due to the overlap of first-order MMRs (Wisdom 1980; Deck et al. 2013; Petit et al. 2018), and a slow crossing of this area would generally result in the excitation of the bodies' eccentricities, leading to collision or scattering instead of the capture into the resonance.

Nevertheless, several formation scenarios of co-orbital configurations can be found in the literature. Laughlin and Chambers (2002) suggested planet-planet gravitational scattering followed by strong eccentricity damping due to the protoplanetary disc, or accretion *in situ* at the L_4/L_5 points of a primary. Alternatively, the presence of an external body such as a massive planet can help the capture of co-orbital bodies through resonant crossing (see Nesvorny et al. 2013, for the case of the solar system).

In the *in situ* scenario, different studies yielded different upper limit to the mass that can form at the L_4/L_5 equilibrium point of a giant planet: Beaugé et al. (2007) obtained a maximum mass of $\sim 0.6 M_\oplus$, while Lyra et al. (2009) obtained $5-15 M_\oplus$ planets in the tadpole area of a Jupiter-mass primary.

Co-orbital pairs form naturally in models of formation of planetary systems (e.g. Cresswell and Nelson 2009; Coleman et al. 2019; Emsenhuber et al. 2021) in typically a few percent of the systems, through scattering, but also during the migration and encounter of resonant chains: in the simulation of the formation of Trappist-1 by Coleman et al. (2019), co-orbitals were mostly found as a part of a resonant chain, which appears to have a stabilising effect (Leleu et al. 2019a). However, models of the formation of planetary systems model the disc-planet interactions using analytical expression computed for single planets. The presence of a co-orbital configuration has been shown to impact significantly the local proto-planetary disc structure, sometime changing the stability of the co-orbital pair (Pierens and Raymond 2014; Leleu et al. 2019a).

Nonetheless, co-orbitals can also form in hydro-dynamical simulations of the proto-planetary disc with two or more planets embedded (e.g. Crida 2009; Penzlin et al. 2019). In several simulations of the formation of the outer part of the solar system, Crida (2009) found that Uranus and Neptune ended up in co-orbital configuration, while being both trapped in the same MMR with Saturn. This reinforces the idea that resonant chains might be favorable to the formation of co-orbital configuration. As long as the planets do not fully open a gap in the proto-planetary disc (typically for planet smaller than Neptune), co-orbitals evolving in the proto-planetary disc appear to be more stable when the leading planet is more massive (Pierens and Raymond 2014; Leleu et al. 2019a), while trailing more massive planet tends to disrupt the configuration. In the case of a terrestrial planet co-orbital with a Jupiter-sized planet, the stability seemed to mainly depend on the proto planetary disc parameters.

For close-in systems, the effect of tides raised by the star onto co-orbital planets appears to always be disruptive (Rodríguez et al. 2013; Couturier et al. 2021; Dobrovolskis and Lissauer 2022). However this phenomenon only impacts planets close to their host star, and most co-orbitals that are at more than 10 days of orbital period at the disc dispersal should survive for billions of years (Couturier et al. 2021).

Detection of co-orbital planets

Stacking the phase-folded lightcurve of thousands of KOIs, Hippke and Angerhausen (2015) found statistical hints of dips near the L_4 and L_5 equilibria of known planets. However, despite the discovery of thousands of exoplanets in hundreds of multiplanetary systems, no extra-solar co-orbital configurations has been confirmed thus far. The subsequent sections discuss the signature of co-orbital configurations in photometric (transit) and spectroscopic (radial velocity) measurements.

Transit

Transit surveys such as Kepler, TESS and the upcoming PLATO mission have discovered the bulk of known exo-planetary systems. As for any other pair of planets, the detection of co-orbitals by transit would require both planets to orbit roughly in the same orbital plane. In addition, their detection requires that each of the co-orbital is large enough for its individual transits to be detected.

For smaller planets, the data-reduction pipelines of transit surveys use an approach similar to the box least square algorithm (BLS, see Kovács et al. 2002; Jenkins et al. 2010, 2016). These algorithms fold each light curve over a large number of different periods and look for transits in the folded data.

This method is adapted to planets on unperturbed or moderately perturbed orbits for which the transits occur periodically. However, gravitational interactions between planets in resonant systems produce transit timing variations (TTVs). Figure 3 shows examples of TTVs for different co-orbital configurations. These TTVs can prevent the detection of small planets if their amplitude σ_{TTV} (amplitude of the oscillation of the curves along the x-axis) is larger than the transit duration D of the planet (width of the curves), and their period is shorter than the mission duration (y-axis). In this case, the signal-to-noise ratio of the transit of the planet recovered by BLS-like algorithms decreases by a factor $1/(1+\sigma_{TTV}/D)$ (Leleu et al. 2021). In addition, the recovered transit shape is altered by the TTVs, and therefore the planet can be missed, or mistaken for a false positive (Leleu et al. 2022).

Assuming that the masses m_p of the two planets are comparable and that it is the same for their eccentricities e_p, a rough calculation (see Gallardo et al. 2021; Nesvorný and Vokrouhlický 2016, and references therein for accurate expressions) shows that, for a MMR of order q, the TTVs occur on a timescale proportional to:

$$P_{TTV} \propto (m_p/m_\star)^{-1/2} e_p^{-q/2} P_{orb}\,. \tag{1}$$

Note that this formula is not singular because the eccentricities cannot be cancelled simultaneously if $q \geq 1$. With $q = 0$, co-orbitals hence generate faster TTVs than other MMRs. In addition their amplitude can be a significant fraction of the orbital period of the planets (e.g. Nesvorný and Vokrouhlický 2014; Leleu et al. 2019b, and Fig. 3). Co-orbitals are hence especially subject to the TTV bias, and dedicated

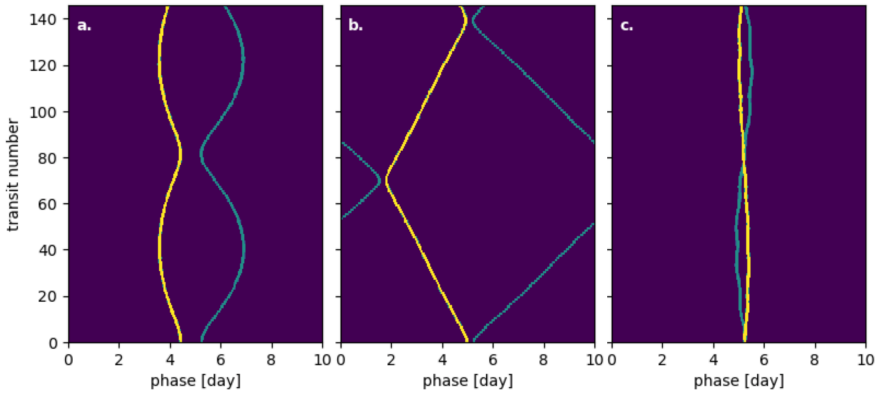

Fig. 3 River diagrams (Carter et al. 2012) for co-orbitals in tadpole orbit (a.), horseshoe orbit (b.) and quasi-satellite (c.). These diagrams show the transit timings of each planet as function of the phase of the average period of the planets (here 10 days, x axis), for each epoch (y axis). In each case, the yellow track shows the transit of the most massive of the two planets, and the blue track shows the transits of the least massive. Assuming a sun-like star, $m_1 = 2m_2 = 10m_\oplus$ for a. and c.; and $m_1 = 2m_2 = 2m_\oplus$ for b.

methods are required to recover potential pairs of small co-orbitals in transit surveys data.

Assuming a large mass discrepancy between co-orbitals, Janson (2013) looked for dips near the L_4 and L_5 equilibrium of known planets, using an analytical model for small libration of the resonant angle and low eccentricities. No significant signal was found, despite a sensitivity level down to Earth-size objects. However, such a signal could still exist for larger amplitudes of libration or eccentricities.

If the co-orbitals are similar in size, both of them could be affected by the TTV bias, in which case both would have been missed by BLS-like approaches, and all orbital periods have to be probed to recover them. The QATS algorithm is adapted to the research of planets with TTVs: it allows the timing of each transit to vary at the same time that it adjusts the best transit depth and duration (Carter and Agol 2013). Alternatively, neural networks trained to recover the track of planets in river diagrams were shown to be capable of detecting planets with large TTVs and low S/N (Leleu et al. 2021, 2022).

Co-orbitals might also be detected even if only one of them transit: with a good phase coverage and high S/N transits, it is possible, based on the TTVs of a single

planet, to determine in which MMR that planet and its perturber are (see the case of KOI-142, Nesvorný et al. 2013). When co-orbitals librate with a significant amplitude the peculiar shape of their TTVs (arches for tadpole-orbits as shows in Fig. 3-a and triangle for horseshoe as shown in Fig. 3-b and in the figure 8 by Vokrouhlický and Nesvorný 2014) could suffice to confirm the existence of a co-orbital configuration.

Radial velocity

Co-orbitals librating in Trojan or horseshoe configurations modulate the radial velocity (RV) signal with a period equal to their libration period. The amplitude of this modulation increases when the mass of the planets tend toward equal value and the amplitude of libration increases (Laughlin and Chambers 2002; Ford and Holman 2007). If this modulation is observed, the estimation of the Keplerian signal and the first modulation harmonics is sufficient to recover the orbit and masses of the planets (Leleu et al. 2015).

For a pair of co-orbital at the exact Lagrangian equilibrium, the modulation vanishes and the generated radial velocities are identical from those induced by a single planet located at their longitudinal barycenter with a mass of $\sqrt{m_1^2+m_2^2+m_1m_2}$, (see Giuppone et al. 2012; Leleu et al. 2017), and hence the co-orbital configuration cannot be identified. However, in the best configuration (equal mass planets, large libration amplitude), the maximum modulation amplitude can be up to $\sim 30\%$ for tadpole orbit and 100% for horseshoe (the RV signal vanishes when the planets are in opposition with respect to the star). In this case, the modulation would be detectable with current radial-velocity instruments. It however requires a long observational baseline to cover the libration period, and might be difficult to disentangle from other dynamical effects or noise. In the case of quasi-satellite orbits, Laughlin and Chambers (2002) remark that the RV signal is also similar to one induced by a single planet, however a small fraction of the orbital phase shows a strong variation in RV.

The co-orbital signature is similar in astrometry. However, the system observed in astrometry tend to be at larger orbital period, making it unlikely to observe a system long enough to see the resonant modulation of the signal.

Radial velocity and transit

Combining RVs and transits allows observers to detect co-orbitals when only one of them transits and without the need to observe the resonant libration. For a single planet in circular orbit, the time of mid-transit coincides with the instant where the radial-velocity reaches its mean value. If the transiting planet has a co-orbital companion, there is a time shift Δt between these two phenomena that depends on

the mass distribution between the co-orbitals and their angular separation ζ (Ford and Gaudi 2006; Leleu et al. 2017). If P is the common orbital period, this time shift reads:

$$\Delta t = \frac{P}{2\pi}\left(\frac{\zeta}{2} - \arctan\left((1-2\delta)\tan\frac{\zeta}{2}\right)\right) \text{ with } \quad \delta = \frac{m_2}{m_1+m_2}, \tag{2}$$

m_1 being the transiting planet mass and m_2 the co-orbital one. But this time shift also exits with a single planet on an elliptic orbit of eccentricity e and argument of pericentre ω. In this case, the time shift reads:

$$\Delta t = -e\cos\omega\frac{P}{2\pi}. \tag{3}$$

The sensibility of this approach hence depends on the precision reached on the quantity $e\cos\omega$ of the transiting planet. So far, this approach could only be used on hot Jupiter, for which the observation of the secondary eclipse can constrain $e\cos\omega$ (Madhusudhan and Winn 2009; Lillo-Box et al. 2018a,b). No co-orbital companion were found in these studies, which is consistent with their instability to tides (Couturier et al. 2021).

Conclusion

Co-orbital exoplanets can be stable for duration longer than the life of their host star if they are sufficiently far away from the star to prevent large tidal disruption, and in the absence of large perturbations by additional planets. In addition, models of formation of planetary systems tend to create pairs of co-orbital exoplanets. However this resonance has several particularities, like that of being surrounded by large chaotic zones, or to modify the local proto-planetary disc structure because of the presence of two planets at the same distance to the star. This require extra care when studying to formation and evolution of co-orbital systems.

Co-orbital exoplanets have not be found yet. However, the methods used to detect the bulk of the exoplanets have biases that impede their capability to recover exoplanets in this kind of configuration. The development of dedicated data analysis methods is required, and the continuous increase in measurement precision and observation baseline could allow us to identify a co-orbital signature in the future. Co-orbitals could also be found by other methods such as direct imaging which, combined with stability studies, has been shown to be able to identify the resonant state of multi-planetary systems (Goździewski and Migaszewski 2020).

References

Beaugé, C., Sándor, Z., Érdi, B., and Süli, Á. (2007). Co-orbital terrestrial planets in exoplanetary systems: a formation scenario. *A&A*, 463:359–367.

Carter, J. A. and Agol, E. (2013). The Quasiperiodic Automated Transit Search Algorithm. *ApJ*, 765(2):132.

Carter, J. A., Agol, E., Chaplin, W. J., Basu, S., Bedding, T. R., Buchhave, L. A., Christensen-Dalsgaard, J., Deck, K. M., Elsworth, Y., Fabrycky, D. C., Ford, E. B., Fortney, J. J., Hale, S. J., Handberg, R., Hekker, S., Holman, M. J., Huber, D., Karoff, C., Kawaler, S. D., Kjeldsen, H., Lissauer, J. J., Lopez, E. D., Lund, M. N., Lundkvist, M., Metcalfe, T. S., Miglio, A., Rogers, L. A., Stello, D., Borucki, W. J., Bryson, S., Christiansen, J. L., Cochran, W. D., Geary, J. C., Gilliland, R. L., Haas, M. R., Hall, J., Howard, A. W., Jenkins, J. M., Klaus, T., Koch, D. G., Latham, D. W., MacQueen, P. J., Sasselov, D., Steffen, J. H., Twicken, J. D., and Winn, J. N. (2012). Kepler-36: A Pair of Planets with Neighboring Orbits and Dissimilar Densities. *Science*, 337:556.

Coleman, G. A. L., Leleu, A., Alibert, Y., and Benz, W. (2019). Pebbles versus planetesimals: the case of Trappist-1. *A&A*, 631:A7.

Couturier, J., Robutel, P., and Correia, A. C. M. (2021). An analytical model for tidal evolution in co-orbital systems. i. application to exoplanets. *Celest. Mech. Dyn. Astron.*

Cresswell, P. and Nelson, R. P. (2008). Three-dimensional simulations of multiple protoplanets embedded in a protostellar disc. *aap*, 482:677–690.

Cresswell, P. and Nelson, R. P. (2009). On the growth and stability of Trojan planets. *Astron. Astrophys.*, 493:1141–1147.

Crida, A. (2009). Minimum Mass Solar Nebulae and Planetary Migration. *ApJ*, 698(1):606–614.

Danby, J. M. A. (1964). Stability of the triangular points in the elliptic restricted problem of three bodies. *Astron. Astrophys.*, 69:165.

Deck, K. M., Payne, M., and Holman, M. J. (2013). First-order Resonance Overlap and the Stability of Close Two-planet Systems. *ApJ*, 774:129.

Delisle, J.-B., Laskar, J., Correia, A. C. M., and Boué, G. (2012). Dissipation in planar resonant planetary systems. *Astron. Astrophys.*, 546:A71.

Dermott, S. F. and Murray, C. D. (1981). The dynamics of tadpole and horseshoe orbits II. The coorbital satellites of saturn. *Icarus*, 48:12–22.

Dobrovolskis, A. R. and Lissauer, J. J. (2022). Do tides destabilize Trojan exoplanets? *Icarus*, 385:115087.

Emsenhuber, A., Mordasini, C., Burn, R., Alibert, Y., Benz, W., and Asphaug, E. (2021). The New Generation Planetary Population Synthesis (NGPPS). I. Bern global model of planet formation and evolution, model tests, and emerging planetary systems. *A&A*, 656:A69.

Érdi, B., Nagy, I., Sándor, Z., Süli, Á., and Fröhlich, G. (2007). Secondary resonances of co-orbital motions. *MNRAS*, 381:33–40.

Euler, L. (1764). Considerationes de motu corporum coelestium. *Novi commentarii academiae scientiarum Petropolitanae. Berlin acad.*, 10:544–558.

Fabrycky, D. C., Lissauer, J. J., Ragozzine, D., Rowe, J. F., Steffen, J. H., Agol, E., Barclay, T., Batalha, N., Borucki, W., Ciardi, D. R., Ford, E. B., Gautier, T. N., Geary, J. C., Holman, M. J., Jenkins, J. M., Li, J., Morehead, R. C., Morris, R. L., Shporer, A., Smith, J. C., Still, M., and Van Cleve, J. (2014). Architecture of Kepler's Multi-transiting Systems. II. New Investigations with Twice as Many Candidates. *apj*, 790:146.

Ford, E. B. and Gaudi, B. S. (2006). Observational Constraints on Trojans of Transiting Extrasolar Planets. *apjl*, 652:L137–L140.

Ford, E. B. and Holman, M. J. (2007). Using Transit Timing Observations to Search for Trojans of Transiting Extrasolar Planets. *apjl*, 664:L51–L54.

Gallardo, T., Beaugé, C., and Giuppone, C. A. (2021). Semianalytical model for planetary resonances. Application to planets around single and binary stars. *A&A*, 646:A148.

Gascheau, G. (1843). Examen d'une classe d'équations différentielles et application à un cas particulier du problème des trois corps. *C. R. Acad. Sci. Paris*, 16(7):393–394.

Giorgilli, A., Delshams, A., Fontich, E., Galgani, L., and Simó, C. (1989). Effective stability for a hamiltonian system near an elliptic equilibrium point, with an application to the restricted three body problem. *JDIFE*, 77(1):167–198.

Giuppone, C. A., Beaugé, C., Michtchenko, T. A., and Ferraz-Mello, S. (2010). Dynamics of two planets in co-orbital motion. *MNRAS*, 407:390–398.

Giuppone, C. A. Benitez-Llambay, P., , and Beaugé, C. (2012). Origin and detectability of co-orbital planets from radial velocity data. *MNRAS*.

Goździewski, K. and Migaszewski, C. (2020). An exact, generalized laplace resonance in the hr 8799 planetary system. *The Astrophysical Journal*, 902(2):L40.

Henrard, J. and Lemaitre, A. (1983). A second fundamental model for resonance. *Celestial Mechanics*, 30:197–218.

Hippke, M. and Angerhausen, D. (2015). Photometrys Bright Future: Detecting Solar System Analogs with Future Space Telescopes. *The Astrophysical Journal*, 810:29.

Holman, M. J. and Wisdom, J. (1993). Dynamical stability in the outer solar system and the delivery of short period comets. *Astron. J.*, 105:1987–1999.

Hou, X. Y., Scheeres, D. J., and Liu, L. (2014). Saturn Trojans: a dynamical point of view. *MNRAS*, 437:1420–1433.

Izidoro, A., Ogihara, M., Raymond, S. N., Morbidelli, A., Pierens, A., Bitsch, B., Cossou, C., and Hersant, F. (2017). Breaking the chains: hot super-Earth systems from migration and disruption of compact resonant chains. *MNRAS*, 470(2):1750–1770.

Janson, M. (2013). A Systematic Search for Trojan Planets in the Kepler Data. *apj*, 774:156.

Jenkins, J. M., Caldwell, D. A., Chandrasekaran, H., Twicken, J. D., Bryson, S. T., Quintana, E. V., Clarke, B. D., Li, J., Allen, C., Tenenbaum, P., Wu, H., Klaus, T. C., Middour, C. K., Cote, M. T., McCauliff, S., Girouard, F. R., Gunter, J. P., Wohler, B., Sommers, J., Hall, J. R., Uddin, A. K., Wu, M. S., Bhavsar, P. A., Van Cleve, J., Pletcher, D. L., Dotson, J. A., Haas, M. R., Gilliland, R. L., Koch, D. G., and Borucki, W. J. (2010). Overview of the Kepler Science Processing Pipeline. *ApJ*, 713:L87–L91.

Jenkins, J. M., Twicken, J. D., McCauliff, S., Campbell, J., Sanderfer, D., Lung, D., Mansouri-Samani, M., Girouard, F., Tenenbaum, P., Klaus, T., Smith, J. C., Caldwell, D. A., Chacon, A. D., Henze, C., Heiges, C., Latham, D. W., Morgan, E., Swade, D., Rinehart, S., and Vanderspek, R. (2016). The TESS science processing operations center. In *Software and Cyberinfrastructure for Astronomy IV*, volume 9913 of *Society of Photo-Optical Instrumentation Engineers (SPIE) Conference Series*, page 99133E.

Kovács, G., Zucker, S., and Mazeh, T. (2002). A box-fitting algorithm in the search for periodic transits. *A&A*, 391:369–377.

Lagrange (1772). *Œuvres complètes*. Gouthier-Villars, Paris (1869).

Laughlin, G. and Chambers, J. E. (2002). Extrasolar Trojans: The Viability and Detectability of Planets in the 1:1 Resonance. *Astron. J.*, 124:592–600.

Lee, M. H. and Peale, S. J. (2002). Dynamics and Origin of the 2:1 Orbital Resonances of the GJ 876 Planets. *ApJ*, 567:596–609.

Leleu, A., Chatel, G., Udry, S., Alibert, Y., Delisle, J. B., and Mardling, R. (2021). Alleviating the transit timing variation bias in transit surveys. I. RIVERS: Method and detection of a pair of resonant super-Earths around Kepler-1705. *A&A*, 655:A66.

Leleu, A., Coleman, G., and Ataiee, S. (2019a). On the stability of the co-orbital resonance under dissipation: Application to the evolution in protoplanetary discs. *arXiv e-prints*, page arXiv:1901.07640.

Leleu, A., Delisle, J. B., Mardling, R., Udry, S., Chatel, G., Alibert, Y., and Eggenberger, P. (2022). Alleviating the Transit Timing Variations bias in transit surveys. II. RIVERS: Twin resonant Earth-sized planets around Kepler-1972 recovered from Kepler's false positive. *arXiv e-prints*, page arXiv:2201.11459.

Leleu, A., Lillo-Box, J., Sestovic, M., Robutel, P., Correia, A. C. M., Hara, N., Angerhausen, D., Grimm, S. L., and Schneider, J. (2019b). Co-orbital exoplanets from close-period candidates: the TOI-178 case. *A&A*, 624:A46.

Leleu, A., Robutel, P., and Correia, A. C. M. (2015). Detectability of quasi-circular co-orbital planets. Application to the radial velocity technique. *Astron. Astrophys.*, 581:A128.

Leleu, A., Robutel, P., and Correia, A. C. M. (2018). On the coplanar eccentric non-restricted co-orbital dynamics. *Celestial Mechanics and Dynamical Astronomy*, 130(3):24.

Leleu, A., Robutel, P., Correia, A. C. M., and Lillo-Box, J. (2017). Detection of co-orbital planets by combining transit and radial-velocity measurements. *Astronomy and Astrophysics*, 599:L7.

Levison, H., Shoemaker, E., and Shoemaker, C. (1997). The long-term dynamical stability of Jupiter's Trojan asteroids. *Nature*, 385:42–44.

Lillo-Box, J., Barrado, D., Figueira, P., Leleu, A., Santos, N. C., Correia, A. C. M., Robutel, P., and Faria, J. P. (2018a). The TROY project: Searching for co-orbital bodies to known planets. I. Project goals and first results from archival radial velocity. *A&A*, 609:A96.

Lillo-Box, J., Leleu, A., Parviainen, H., Figueira, P., Mallonn, M., Correia, A. C. M., Santos, N. C., Robutel, P., Lendl, M., Boffin, H. M. J., Faria, J. P., Barrado, D., and Neal, J. (2018b). The TROY project. II. Multi-technique constraints on exotrojans in nine planetary systems. *A&A*, 618:A42.

Lyra, W., Johansen, A., Klahr, H., and Piskunov, N. (2009). Standing on the shoulders of giants. Trojan Earths and vortex trapping in low mass self-gravitating protoplanetary disks of gas and solids. *aap*, 493:1125–1139.

Madhusudhan, N. and Winn, J. N. (2009). Empirical Constraints on Trojan Companions and Orbital Eccentricities in 25 Transiting Exoplanetary Systems. *ApJ*, 693:784–793.

Marzari, F., Tricarico, P., and Scholl, H. (2003). Stability of jupiter trojans investigated using frequency map analysis: the matros project. *MNRAS*, 345:1091–1100.

Morais, M. H. M. and Namouni, F. (2016). A numerical investigation of coorbital stability and libration in three dimensions. *Celestial Mechanics and Dynamical Astronomy*, 125(1):91–106.

Namouni, F. (1999). Secular Interactions of Coorbiting Objects. *Icarus*, 137:293–314.

Nauenberg, M. (2002). Stability and Eccentricity for Two Planets in a 1:1 Resonance, and Their Possible Occurrence in Extrasolar Planetary Systems. *Astron. J.*, 124:2332–2338.

Nesvorny, D. and Dones, L. (2002). How long-live are the hypothetical Trojan populations of Saturn, Uranus, and Neptune? *Icarus*, 160:271–288.

Nesvorný, D., Kipping, D., Terrell, D., Hartman, J., Bakos, G. Á., and Buchhave, L. A. (2013). KOI-142, The King of Transit Variations, is a Pair of Planets near the 2:1 Resonance. *ApJ*, 777(1):3.

Nesvorný, D. and Vokrouhlický, D. (2014). The Effect of Conjunctions on the Transit Timing Variations of Exoplanets. *ApJ*, 790(1):58.

Nesvorný, D. and Vokrouhlický, D. (2016). Dynamics and Transit Variations of Resonant Exoplanets. *ApJ*, 823(2):72.

Nesvorny, D., Vokrouhlicky, D., and Morbidelli, A. (2013). Capture of Trojans by Jumping Jupiter. *APJ*, 768:45.

Papaloizou, J. C. B. and Terquem, C. (2010). On the dynamics of multiple systems of hot super-Earths and Neptunes: tidal circularization, resonance and the HD 40307 system. *MNRAS*, 405(1):573–592.

Penzlin, A. B. T., Ataiee, S., and Kley, W. (2019). 1:1 orbital resonance of circumbinary planets. *A&A*, 630:L1.

Petit, A. C., Laskar, J., and Boué, G. (2018). Hill stability in the AMD framework. *A&A*, 617:A93.

Pierens, A. and Raymond, S. N. (2014). Disruption of co-orbital (1:1) planetary resonances during gas-driven orbital migration. *mnras*, 442:2296–2303.

Pousse, A., Robutel, P., and Vienne, A. (2017). On the co-orbital motion in the planar restricted three-body problem: the quasi-satellite motion revisited. *Celestial Mechanics and Dynamical Astronomy*.

Pu, B. and Wu, Y. (2015). Spacing of Kepler Planets: Sculpting by Dynamical Instability. *ApJ*, 807:44.

Qi, Y. and de Ruiter, A. (2020). Phase Structure of Co-orbital Motion with Jupiter. *MNRAS*.

Roberts, G. (2002). Linear stability of the elliptic Lagrangian triangle solutions in thethree-body problem. *JDIFE*, 182:191–218.

Robutel, P. and Gabern, F. (2006). The resonant structure of Jupiter's Trojan asteroids I: Long-term stability and diffusion. *MNRAS*, 372:1463–1482.

Rodríguez, A., Giuppone, C. A., and Michtchenko, T. A. (2013). Tidal evolution of close-in exoplanets in co-orbital configurations. *Celest. Mech. Dyn. Astron.*, 117:59–74.

Sidorenko, V. V., Neishtadt, A. I., Artemyev, A. V., and Zelenyi, L. M. (2014). Quasi-satellite orbits in the general context of dynamics in the 1:1 mean motion resonance: perturbative treatment. *Celestial Mechanics and Dynamical Astronomy*, 120(2):131–162.

Terquem, C. and Papaloizou, J. C. B. (2007). Migration and the Formation of Systems of Hot Super-Earths and Neptunes. *ApJ*, 654(2):1110–1120.

Thomas, P. C., Burns, J. A., Hedman, M., Helfenstein, P., Morrison, S., Tiscareno, and Veverka, J. (2013). The inner small satellites of saturn: A variety of worlds. *Icarus*, 226(999–1019).

Vokrouhlický, D. and Nesvorný, D. (2014). Transit Timing Variations for Planets Co-orbiting in the Horseshoe Regime. *ApJ*, 791:6.

Wisdom, J. (1980). The resonance overlap criterion and the onset of stochastic behavior in the restricted three-body problem. *Astrophysical Journal*, 85:1122–1133.

Wolf, M. (1906). Photographische Aufnahmen von kleinen Planeten. *Astronomische Nachrichten*, 170:353.